frontiers | Frontiers in Physics

TYPE Brief Research Report
PUBLISHED 15 May 2023
DOI 10.3389/fphy.2023.1208411

Check for updates

OPEN ACCESS

EDITED BY
Zhenxu Bai,
Hebei University of Technology, China

REVIEWED BY
Zhichao Liu,
Changchun University of Science and Technology, China
Mingming Luo,
Hebei University of Technology, China

*CORRESPONDENCE
Dajun Chang,
changdajun@mails.cust.edu.cn

RECEIVED 19 April 2023
ACCEPTED 05 May 2023
PUBLISHED 15 May 2023

CITATION
Chang Y, Chang D and Su L (2023), Based on adaptive modulation laser communication multi-microgrids scheduling system.
Front. Phys. 11:1208411.
doi: 10.3389/fphy.2023.1208411

COPYRIGHT
© 2023 Chang, Chang and Su. This is an open-access article distributed under the terms of the Creative Commons Attribution License (CC BY). The use, distribution or reproduction in other forums is permitted, provided the original author(s) and the copyright owner(s) are credited and that the original publication in this journal is cited, in accordance with accepted academic practice. No use, distribution or reproduction is permitted which does not comply with these terms.

Based on adaptive modulation laser communication multi-microgrids scheduling system

Ying Chang[1], Dajun Chang[2]* and Li Su[3]

[1]School of Computer Engineering and Artificial Intelligence, Jilin University of Architecture and Technology, Changchun, Jilin, China, [2]School of Electrical Information, Changchun University of Architecture and Civil Engineering, Changchun, Jilin, China, [3]Jilin Academy of Chinese Medicine Sciences, Changchun, Jilin, China

In order to improve the data sharing and comprehensive information processing capabilities between multi-microgrids in the power system, the multi-microgrids scheduling system based on laser communication has been proposed. In order to reduce the error rate of laser communication and reduce the impact of atmospheric turbulence on signal acquisition, an adaptive modulation algorithm has been designed. A mathematical model for laser communication modulation and demodulation based on adaptive modulation algorithm has been constructed. In simulation analysis, the target signal was extracted from the original signal superimposed with atmospheric turbulence noise through filtering and demodulation. The energy fluctuation of the extracted signal decreased from 47.3 to 5 mV. The energy attenuation trend of communication lasers within the range of 0–6 km was experimentally tested. Within 2.0 km, the energy demodulation results of both algorithms are similar, both below 10%. After exceeding 2.0 km, the calculation error of the adaptive modulation algorithm remains basically unchanged, while the error of traditional algorithms increases by about twice. For the APD response value, the adaptive modulation algorithm demodulation has a higher response range concentration ratio and the higher envelope recognition. Under different nominal atmospheric turbulence values, the maximum error rates of the adaptive modulation algorithm are 5.8×10^{-8}, 8.9×10^{-8}, and 1.2×10^{-7}, respectively, while the maximum error rates of the amplitude coherent algorithm are 2.9×10^{-5}, 6.3×10^{-5}, and 1.05×10^{-4}, respectively. It can effectively suppress the impact of atmospheric turbulence on the error rate of laser communication by adaptive modulation algorithm.

KEYWORDS

laser communication, multi-microgrids scheduling, adaptive modulation, error rate, demodulation analysis

1 Introduction

With the development of the Internet and microgrids technology, a single microgrid is no longer able to meet existing energy needs. In order to improve the reliability of large-scale power supply, sub-microgrids are constructed into interconnected and interconnected multi-microgrids systems [1]. "Internet plus + multi micro network" can realize the intelligence of energy, and realize the comprehensive management of energy storage, energy transmission and energy use through big data, cloud computing and other technologies [2]. A multi-microgrids

system can achieve reliable power supply for multiple loads, and by combining micro sources, multiple sources can complement each other and improve energy utilization efficiency. The coordinated control technology of Internet plus multi-microgrids connection is one of the important research directions [3]. In order to achieve efficient communication of multi-microgrids data, laser communication technology is used to construct high-speed data communication transmission channels in the multi-microgrids system.

With the continuous maturity of equipment such as lasers, detectors, and optical amplifiers, laser communication technology has also made significant progress in the civilian field. In 2017, Ratnam V [4] completed laser communication experiments between airships using an FSOC optical transceiver. Its communication distance exceeds 100 km and communication rate is 130Mbps. In 2018, Horwath [5] used airborne terminals MLT-70 and GS-200 ground stations to achieve communication, with a communication rate of up to 10Gbps and a communication distance of 10 km. In 2018, Hu H [6] completed laser communication between vehicles using a 15ZFF optical transceiver, with a central wavelength of 1550 nm. At a distance of 0.5km, the communication rate is 2.5Gbps. At a distance of 10km, the communication rate is 155Mbps. In 2019, Li L [7] completed laser communication experiments between buildings using an Artolink optical transceiver. In the experiment, a 1550 nm laser was used, with a system link distance of 4.4 km and a communication rate of 1.25Gbps. In 2019, Sayan O F [8] completed laser communication between aircraft using the MLT-30 optical transceiver, with a communication link of up to 40 km and a communication rate of 10Gbps. In 2019, Von Rhein J [9] used a 15YDF optical transceiver for malicious communication between two buildings, with a communication distance of 500 m and a communication speed of 10Gbps. In 2020, Yu X [10] used a full cycle laser terminal for real-time communication of 12.7 km dynamic targets, and the system adopted a full cycle dynamic servo mechanism, with a communication rate of up to 2.5Gbps. In 2021, Quintana C [11] conducted laser communication between ground and unmanned aerial vehicles, constructing a data link through the combination of modulators and reflectors. The system has achieved an effective aperture of 11mm, with a communication rate of up to 500Mbps and an error rate of 7.6E-4 over a testing distance of 560 m. In 2023, Chen Hui [12] completed the measurement of Brillouin scattering in laser communication. In 2023, Jin D [13] achieved precise control of modulation frequency by using a narrow linewidth laser modulation. In 2023, Bai Z [14] achieved laser amplitude modulation using a tunable pulse width oscillator, improving the stability of laser communication.

In summary, laser communication has the advantages of large communication capacity and no electromagnetic interference in laser signals. It is very suitable for massive data calculation and communication between multiple microgrids. Therefore, this article proposes a multi micro network networking system based on laser communication.

2 Multi-microgrids scheduling system with laser communication

The multi-microgrids scheduling system based on laser communication is shown in Figure 1. The electrical energy of the main power grid is transmitted to various electricity consuming units through Power transmission lines. The power generation department also transmits electrical energy to the Energy storage system through the main power grid. The load end includes industrial power units, urban power units, etc. All modules use Transformers to complete current matching and circuit breakers to complete circuit protection before being connected to the main power grid. The main information such as power consumption of each output and input unit will be transmitted to the LCU (Laser communication unit) through Data communication. Lidar sends data information from the power microgrids to another. After summarizing all electrical energy transmission information, it is transmitted by the microgrids management system to the Power Grid dispatch center, ultimately completing control of power network distribution, grid connection, etc. In the system, LiDAR can not only achieve data interaction between sub units and the main control unit, but also complete data communication between sub units. Each laser communication unit can be a power data communication terminal in an industrial factory area or a power data communication terminal in an urban area.

The Laser communication unit mainly includes atmospheric channels, lasers, detectors, optical antennas, terminal equipment, power supplies, etc. The information is controlled by the processing system and modulated onto the optical carrier generated by the laser using a modulator. Then transmit it to the receiving end through an optical transmitting antenna. The optical signal reaches the receiving end through an atmospheric channel. The optical receiving antenna focuses the laser signal, which is then converted into an electrical signal by the detector. After amplification and filtering, it enters the processing system of the receiving end.

3 Adaptive laser modulation model

Due to the fact that there is more than one communication location in the power network, the entire system is a laser communication network. For networks, the order of communication between laser communication modules, channel occupancy ratio, and communication time allocation can have an impact on communication efficiency. So in the process of laser communication, it is necessary to adaptively modify the modulation degree and demodulation method under different distances and atmospheric turbulence interference conditions. The adaptive algorithm proposed in this article is to improve the efficiency of laser communication by introducing adaptive parameters during the modulation process.

3.1 Signal expression

In order to achieve higher communication efficiency [15] and reduce the error rate of laser communication, a mathematical model based on adaptive laser modulation was constructed. The signal sequence can be represented by the state values of 1 and 0, that is, 1 and 0 in the carrier amplitude. Firstly, set the main data parameters in the system.

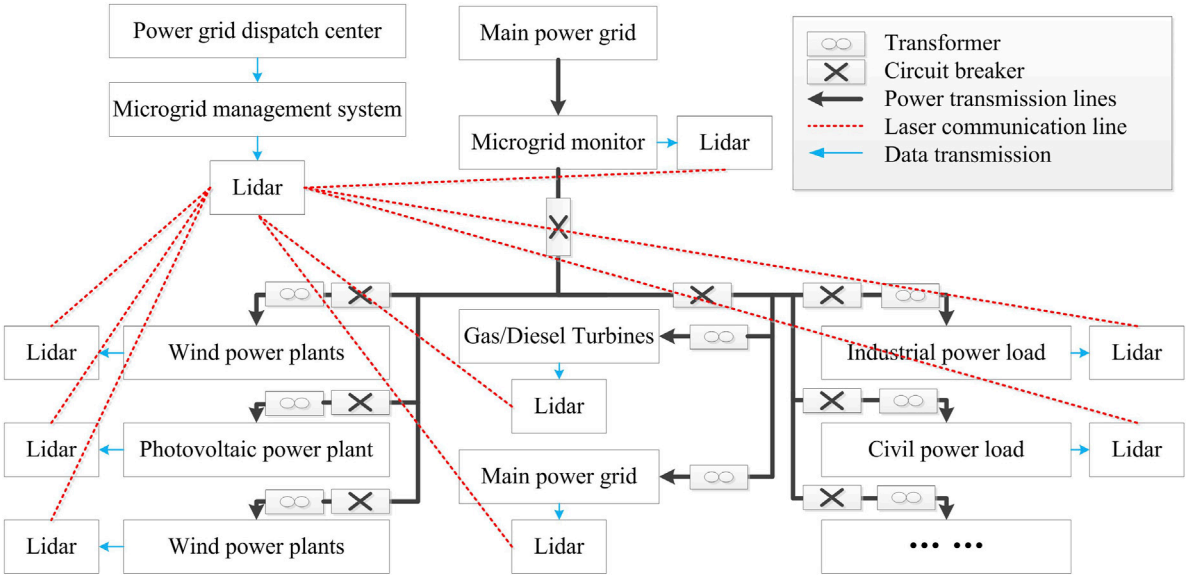

FIGURE 1
Power microgrids monitoring system by laser communication.

a) Signal amplitude. The data amplitude modulation in laser communication is achieved by modulating the basic signal [16], and its formula is as follows

$$V(x) = \sum_i x_i h(x - kX_i) \tag{1}$$

Among them, x_i is the amplitude of ith signal. X_i is the period. $h(x)$ is the pulse waveform. k is the compensation coefficient within the cycle.

b) Frequency shift signal and phase shift signal. Frequency shift signal is the carrier wave of information achieved by the system by overlaying signals of different frequencies [17]. A phase shift signal is the phase shift of a signal. Let the two communication states be 0 and 1, where 0 represents the basic carrier frequency f_1 and 1 represents the carrier frequency f_2. The frequency shift signal and phase shift signal have

$$\begin{cases} Q_f(x) = G\sum_i (x - kX_i)^{\phi_i} \\ Q_p(x) = G\sum_i (x - kX_i)^{\phi - \phi_i} \end{cases} \tag{2}$$

Among them, G is the amplitude. φ is the initial phase. φ_i is the phase of ith test position.

3.2 Modulation model design

Set the power data in the power communication process as the modulation signal $f(x)$, and the carrier signal as $e(x) = \cos\alpha_0 x$, where α_0 is the carrier frequency [18]. The output signal $y(x)$ of the system can be expressed as

$$y(x) = f(x)\cos\alpha_0 x \tag{3}$$

According to Eq. 1, there is a proportional relationship between y x) and f x), which is the amplitude modulation of the laser signal [16]. According to the frequency domain convolution calculation, its spectral expression is

$$Y(i\alpha) = \frac{1}{2\pi} F(i\alpha)^* E(i\alpha) \tag{4}$$

$F(i\alpha)$ and $E(i\alpha)$ can be modulated to achieve signal loading and parsing. The spectrum $Y(i\alpha)$ of y(x) will generate a controllable frequency shift during modulation, which can be automatically aligned during laser communication through adaptive algorithms. The sideband signal in the system can be represented as

$$c(x) = kf(x)\cos\alpha_i x \tag{5}$$

Among them, k represents the processing coefficient. The above formula can suppress noise entering the communication system and achieve real-time adjustment of the system sideband signal amplitude [19]. In order to enable the communication system to automatically switch communication targets in different subunits, an adaptive function is set to classify communication data. The setting parameters for classification are achieved by adding a high pass filtering module, and modifying the filter to perform secondary processing on the updated signal. Set the noise phase shift of the signal in the subunit as an independent state parameter, which has a uniformly distributed feature in the signal interval. Then, calculate the phase offset of different units through processing functions, and obtain the phase setting value for the optimal overall communication. In sub unit communication, initialize the setting data of the processing function. Then, the preset modulation parameters are substituted into the system to complete the adaptive iterative calculation. Finally, the parameter settings that match the overall communication optimal solution will be combined as the updated control parameters.

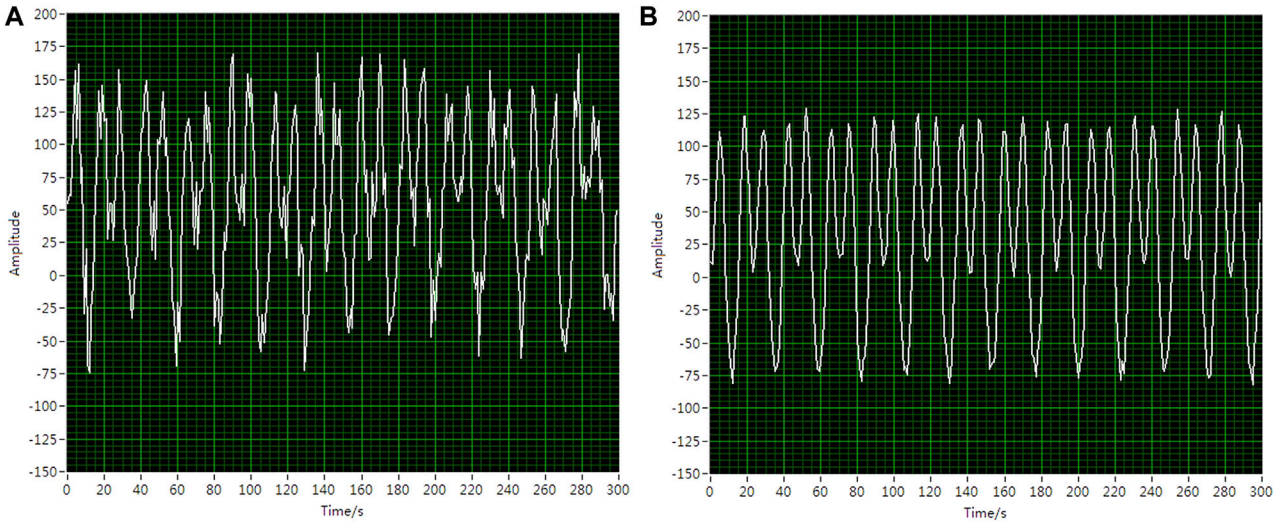

FIGURE 2
Signal curve before and after filtering.

4 Filter simulation analysis

When laser communication is completed between mult-microgrids, communication data will be attenuated in the atmospheric transmission channel, and stray light will interfere with the reception of laser signals. However, due to the significant difference in frequency between other interference signals such as stray light and the modulation signal of the system, the adaptive laser modulation algorithm proposed in this article can be used for filtering. Filter and process the loaded noise signal through Labview. The root mean square value of the noise is 200.0 mV, and the root mean square value of the signal source is 250.0 mV. The noise reduction filtering in this article adopts the built-in filtering program in Labview software, namely, the Cutoff function. Select its bandpass function and set the frequency to 10–100 Hz. Analyze two sets of superimposed signals and extract modulated signals from the mixed signals. The mixed signal and the signal is shown in Figure 2.

As shown in Figure 2A, the laser modulation signal emitted by the laser communication system is affected by atmospheric attenuation and atmospheric turbulence when passing through the atmospheric channel, and the signal will mix with noise, mainly Gaussian white noise. During the simulation, the root mean square value of the noise was set to 200.0 mV, indicating that the modulation waveform experienced peak to peak bifurcation and signal mean shift. The average value of the entire test curve was 58.5 mV, with fluctuations of approximately 47.3 mV. If this signal is directly used for demodulation, it will result in a significant increase in the error rate of the communication system. Therefore, the original signal needs to be filtered first, and the modulated waveform after processing is shown in Figure 2B. The laser modulation signal becomes smooth, and there is no longer a bifurcation phenomenon at each peak position, presenting a single main peak waveform. The average of the entire test curve is 52.3 mV, with fluctuations of less than 5.0 mV, which is about an order of magnitude lower than before optimization. The overall mean shift is very small, and the signal output is stable. Throughout the entire communication process, the error changes of all sampling point test data are basically consistent with it.

5 Experiments

The experimental system includes a laser, a modulation and transmission module, and a reception and demodulation module. The laser adopts Lumileds' c-band infrared laser, with a luminous power superior to 300 mW and a divergence angle of 100 at a communication rate of 10.0Mbps. The collimator adopts the RC08FC collimation system from THORLABS company, with a transmission power of −3.38dBm. The adaptive modulation galvanometer adopts OIM103 electromagnetic galvanometer, with a control voltage of 0- ± 10 V and a maximum rotation amplitude of 25.3 mrad. The APD detector uses the S8664 photoelectric sensor from Hamamatsu Company, with a detection bandwidth of 20Mbps. The AD7605 AD chip is selected in the signal acquisition module to complete rapid data processing.

5.1 Communication laser energy testing

In the process of laser communication, the communication distance has the most significant impact on the communication effect. On the one hand, as the communication distance increases, the degree of spot divergence increases, resulting in a decrease in received laser energy and a decrease in signal-to-noise ratio. On the other hand, the longer the distance through the atmospheric channel, the more obvious the effect of atmospheric disturbances and turbulence. In order to verify the better communication capability of the laser communication system based on adaptive modulation, the same system hardware is used to receive the same

TABLE 1 Laser energy test data under different communication distances.

Test distance (*km*)	TH-M900HDJG (*mA*)	Adaptive modulation algorithm (*mA*)	Error (%)	Amplitude coherence algorithm (*mA*)	Eror (%)
0.5	43.55	41.36	5.03	40.36	7.32
1.0	35.61	33.58	5.70	32.58	8.32
1.5	28.89	27.69	4.15	25.89	9.46
2.0	20.36	18.95	6.93	18.25	9.84
2.5	16.57	16.85	1.69	14.15	14.60
3.0	12.35	11.48	7.04	10.48	15.14
3.5	9.48	8.81	7.07	7.81	17.62
4.0	6.35	5.79	8.82	5.19	18.27
4.5	3.64	3.31	9.07	2.91	20.05
5.0	0.52	0.47	6.77	0.41	21.15
5.5	0.26	0.24	8.69	0.21	23.56
6.0	0.11	0.09	9.25	0.07	24.35

set of laser test signals, and the adaptive modulation algorithm and amplitude coherence algorithm are respectively used for analysis. The test results are shown in Table 1.

The test results show that the received optical power conforms to the logarithmic normal distribution within 2.0 km. Its energy is mainly distributed in the range of 20–40 mA, with a variance of approximately 0.0825. After adopting adaptive modulation, the optical power tends to stabilize, with its energy mainly distributed in the range of 20–25 mA, and the variance reduced to 0.0064. Experiments have shown that adaptive modulation can effectively suppress signal power fluctuations caused by turbulence. Within the range of 2.0–6.5 km, the output optical power of APD exhibits a negative exponential distribution. Its energy is mainly distributed in the range of 0.5–20.0 mA, with a variance of approximately 0.9258. Compared to the test results below 2.0 km, it can be seen that there is energy attenuation and the fluctuation has increased by nearly an order of magnitude. As the communication distance increases, the energy of the communication laser weakens and the variance fluctuation significantly increases. The signal energy calculation results of the two algorithms are similar within 3.0 km. After exceeding 3.0 km, the solution performance of the adaptive modulation algorithm gradually outperforms that of the amplitude coherence algorithm. The testing of laser energy is to analyze the signal amplitude during laser communication, as it is proportional to the laser energy.

5.2 Signal demodulation analysis

In order to verify the good demodulation performance of the adaptive modulation algorithm signal, demodulation analysis was conducted on the laser signal at the receiving end. The signal was obtained using the receiving module in the laser communication system, and 600s of test data were intercepted, as shown in Figure 3.

As shown in Figure 3, the original signal (blue curve in the figure) contains a large amount of noise after passing through the atmospheric channel. The response current fluctuation range on the APD detector is 5–70 mA, with an average of about 38.5 mA and a large variance. After filtering, the filtered signal can be obtained through the demodulation calculation of the adaptive modulation algorithm (red curve in the figure). After filtering and demodulation calculation, the response current fluctuation range on the APD detector is reduced to 22.0–53.0 mA, with an average of about 39.3 mA and a significant reduction in variance. The APD response current demodulated using an adaptive modulation algorithm has good output characteristics. The curve can roughly see the signal envelope in the range of about 100 s, and after data processing, the modulated data can be well recognized. By performing Fourier transform on filtered signals, their frequency domain information can be obtained, and their Frequency shift signal and Phase shift signal can be solved. By comparing with the original modulated signal of the laser communication signal, the frequency shift signal and phase shift signal of the received signal relative to the original signal can be calculated.

5.3 Error rate comparison test

From the received light intensity and the response current of the APD detector, it can be seen that the signal-to-noise ratio has been improved after adopting adaptive modulation. In order to further validate the advantages of this design in laser communication, the error rate of the adaptive modulation algorithm and the amplitude coherence algorithm under different atmospheric turbulence nominal values were compared. The nominal values of atmospheric turbulence are taken as $C_1 = 10^{-15}$, $C_2 = 10^{-16}$ and $C_3 = 10^{-17}$, respectively, and the test results are shown in Figure 4. C_1, C_2 and C_3 are the error rate of a laser communication system, calculated by subtracting the total amount of communication data

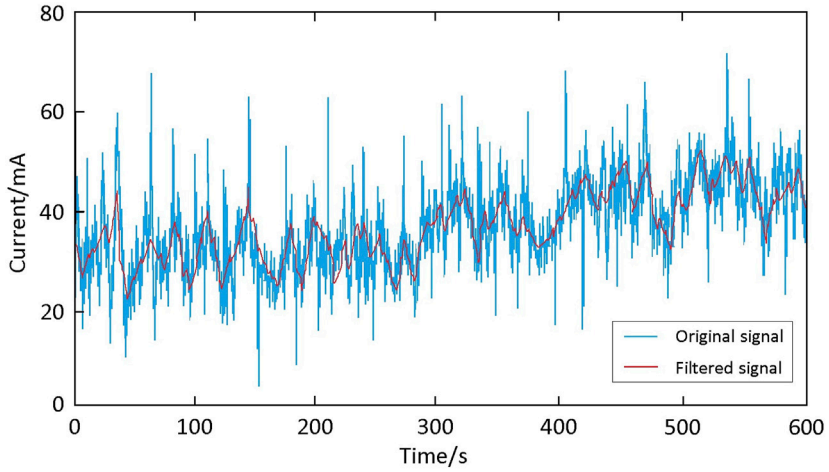

FIGURE 3
APD response current value before and after filtering.

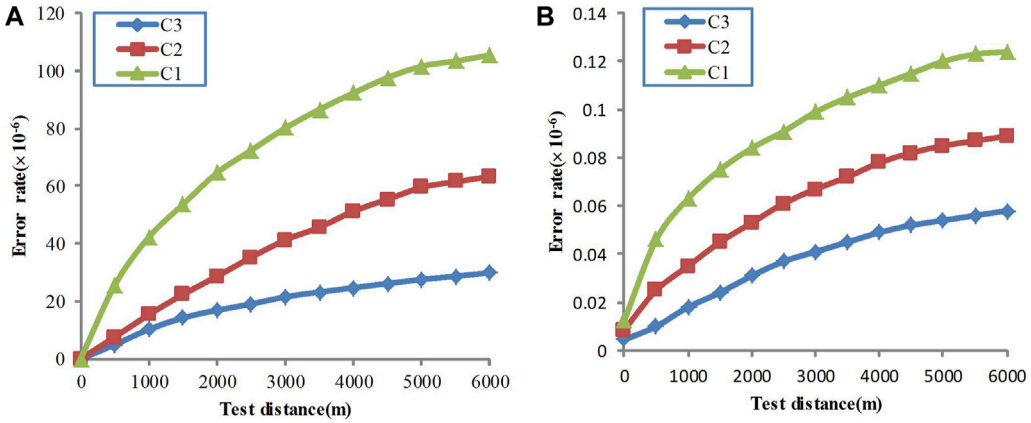

FIGURE 4
Bit error rates before and after adaptive modulation optimization.

from the amount of error data during the communication process and dividing it by the total amount of communication. It is often used to analyze the transmission accuracy of communication systems.

As shown in Figure 4A, as the communication distance increases, the error rate also increases. The testing distance has increased from 0 to 6 km. When $C_1 = 10^{-15}$, the error rate increases from 4.5×10^{-9} to 2.9×10^{-5}; When $C_2 = 10^{-16}$, the bit error rate increases from 8.5×10^{-9} to 6.3×10^{-5}. When $C_3 = 10^{-17}$, the error rate increases from 1.3×10^{-8} to 1.05×10^{-4}. As the nominal value of atmospheric turbulence decreases, the error rate of laser communication systems is also gradually decreasing. In contrast, when $C_1 = 10^{-15}$, the bit error rate using adaptive modulation algorithms increases from 4.3×10^{-9} to 5.8×10^{-8}; When $C_2 = 10^{-16}$, the bit error rate increases from 8.2×10^{-9} to 8.9×10^{-8}. When $C_3 = 10^{-17}$, the error rate increases from 1.2×10^{-8} to 1.2×10^{-7}. The error rate variation amplitude of the adaptive modulation algorithm is much smaller than the calculation result of the amplitude coherence algorithm. The error rate of the adaptive modulation algorithm is also less disturbed by the nominal value of atmospheric turbulence than that of the amplitude coherence algorithm. The superiority of this algorithm has been verified.

6 Conclusion

This article focuses on the problem of requiring a large amount of data transmission in the multi-microgrids scheduling process of power systems, and designs a multi-microgrids scheduling system based on laser communication. Apply adaptive modulation algorithms in laser communication systems to modulate and demodulate communication signals. The impact of atmospheric

turbulence on communication laser energy, APD response value, and laser communication error rate was analyzed through simulation and experimental testing. We compared the testing results of adaptive modulation algorithm and amplitude coherence algorithm, analyzed the error rate of laser communication in different states, and verified the feasibility of the system and the superiority of the algorithm.

Data availability statement

The original contributions presented in the study are included in the article/supplementary material, further inquiries can be directed to the corresponding author.

Author contributions

YC proposed the design concept of the paper and wrote it. DC completed the simulation analysis. LS participated in the experimental testing. All authors contribute to the paper. All authors listed have made a substantial, direct, and intellectual contribution to the work and approved it for publication.

Funding

This work was supported in part by Key R&D of Jilin Provincial Department of Science and Technology, project name: "Research on Key Technologies for Multi-microgrids Connection and Coordinated Control" (20230203050SF).

Conflict of interest

The authors declare that the research was conducted in the absence of any commercial or financial relationships that could be construed as a potential conflict of interest.

Publisher's note

All claims expressed in this article are solely those of the authors and do not necessarily represent those of their affiliated organizations, or those of the publisher, the editors and the reviewers. Any product that may be evaluated in this article, or claim that may be made by its manufacturer, is not guaranteed or endorsed by the publisher.

References

1. Vali Z, Gholami A, Ghassemlooy Z, Michelson DG System parameters effect on the turbulent underwater optical wireless communications link. *Optik* (2019) 198:163153. doi:10.1016/j.ijleo.2019.163153

2. Akyildiz IF, Pompili D, Melodia T. Challenges for efficient communication in underwater acoustic sensor networks. *ACM SIGBED Rev* (2004) 1(2):3–8. doi:10.1145/1121776.1121779

3. Kim J, Joe H, Yu SC, Lee JS, Kim M. Time-delay controller design for position control of autonomous underwater vehicle under disturbances. *IEEE Trans Ind Electron* (2016) 63(2):1052–61. doi:10.1109/tie.2015.2477270

4. Ratnam V, Krishnan P. Bit error rate analysis of ground-to-high altitude platform free-space optical communications using coded polarization shift keying in various weather conditions[J]. *Opt Quan Electron* (2022) 54(1):1–18. doi:10.1007/s11082-021-03398-6

5. Horwath J, Diaz Gonzalez D, Martin Navajas L, Souto AL, Haque F, Grier A, et al. Test results of error-free bidirectional 10 Gbps link for air-to-ground optical communications. In: Free-Space Laser Communication and Atmospheric Propagation XXX; 29-30 January 2018; San Francisco, California, USA. San Jose, California, USA: SPIE (2018).

6. Hu H, Oxenlowe LK, Morioka T, Yankov MP, Da Ros F, Amma Y, et al. Ultrahigh-spectral-efficiency WDM/SDM transmission using PDM-1024-QAM probabilistic shaping with adaptive rate. *J lightwave Technol* (2018) 36(6):1304–8. doi:10.1109/jlt.2017.2787340

7. Li L, Zhang R, Liao P, Cao Y, Song H, Zhao Y, et al. Mitigation for turbulence effects in a 40-Gbit/s orbital-angular-momentum-multiplexed free-space optical link between a ground station and a retro-reflecting UAV using MIMO equalization. *Opt Lett* (2019) 44(21):5181–4. doi:10.1364/ol.44.005181

8. Sayan OF, Gercekcioglu H, Baykal Y. Hermite Gaussian beam scintillations in weak atmospheric turbulence for aerial vehicle laser communications. *Opt Commun* (2020) 458:124735. doi:10.1016/j.optcom.2019.124735

9. Von Rhein J, Henze GP, Long N, Fu Y. Development of a topology analysis tool for fifth-generation district heating and cooling networks. *Energ Convers Manage* (2019) 196(9):705–16. doi:10.1016/j.enconman.2019.05.066

10. Yu X, Zhang L, Zhang Y, Song Y, Tian M, Wang T, et al. 2.5Gbps free-space optical transmission between two 5G airship floating base stations at a distance of 12km. *Opt Lett* (2021) 46(9):2156–2159. doi:10.1364/ol.419690

11. Quintana C, Wang Q, Jakonis D, Oberg O, Erry G, Platt D, et al. A high speed retro-reflective free space Optics links with UAV. *J Lightwave Technol* (2021) 39(18):5699–705. doi:10.1109/jlt.2021.3091991

12. Hui C, Bai Z, Cai Y, Yang X, Ding J, Qi Y, et al. Order controllable enhanced stimulated Brillouin scattering utilizing cascaded diamond Raman conversion. *Appl Phys Lett* (2023) 122(9):092202. doi:10.1063/5.0137542

13. Jin D, Bai Z, Lu Z, Fan R, Zhao Z, Yang X, et al. 22.5-W narrow-linewidth diamond Brillouin laser at 1064 nm. *Opt Lett* (2022) 47(20):5360–5363. doi:10.1364/ol.471447

14. Bai Z, Zhao C, Gao J, Chen Y, Li S, Li Y, et al. Optical parametric oscillator with adjustable pulse width based on KTiOAsO4. *Opt Mater* (2023) 136:113506. doi:10.1016/j.optmat.2023.113506

15. Jin D, Bai Z, Li M, Yang X, Wang Y, Mildren RP, et al. Modeling and characterization of high-power single frequency free-space Brillouin lasers. *Opt Express* (2023) 31(2):2942–2955. doi:10.1364/oe.476759

16. Chen B, Bai Z, Hun X, Wang J, Cui C, Qi Y, et al. Gain characteristics of stimulated Brillouin scattering in fused silica. *Opt Express* (2023) 31(4):5699–5707. doi:10.1364/oe.480391

17. Lin Y Application of neural network-based nonlinear intelligent control in electro-optical tracking systems. *Opt Precision Eng* (2018) 26(12):2949–55. doi:10.3788/ope.20182612.2949

18. Talmora G, Harding JH, Chen CC. Two –axis gimbal for air-to-air and air-to-ground laser communications. *Proc 2016 SPIE* (2016) 9739:1–8. Baltimore. SPIE. doi:10.1117/12.2218097

19. Yang JS. Design and implementation of large scale internet of things laser communication system. *Laser J* (2019) 40(4):92–96.